Available online at www.sciencedirect.com

ScienceDirect

J Materiomics 1 (2015) 285–295

www.ceramsoc.com/en/

www.journals.elsevier.com/journal-of-materiomics/

# An overview of materials issues in resistive random access memory

Linggang Zhu [a,b], Jian Zhou [a], Zhonglu Guo [b], Zhimei Sun [a,b,*]

[a] School of Materials Science and Engineering, Beihang University, Beijing 100191, China

[b] Center for Integrated Computational Materials Engineering, International Research Institute for Multidisciplinary Science, Beihang University, Beijing 100191, China

Received 31 May 2015; revised 4 July 2015; accepted 23 July 2015
Available online 30 July 2015

**Abstract**

Resistive random access memory (RRAM) is a very promising next generation non-volatile RAM, with quite significant advantages over the widely used silicon-based Flash memories. For RRAM, material with switchable resistance, working as the storage medium, is the most important part for the performance of the memory. In this review, as a start, some general hints for the materials selection are proposed. Then most recent studies on this emerging memory from the perspective of materials science are summarized: various materials with resistance switch (RS) behavior and the underlying mechanisms are introduced; as a complementary to the previous review articles, here the increasingly important role of computational materials science in the research of RRAM is presented and highlighted. By incorporating the framework of high-throughput calculation and multi-scale simulations, design process of new RRAM could be accelerated and more cost-effective.


*Keywords:* Resistive random access memory (RRAM); Material selection; Mechanism; Computational material science

## 1. Introduction

With the rapid advances of electronic technology and devices, higher-speed and denser memories are required [1]. Non-volatile memory (NVM) is a type of memory mainly for relatively long-term storage, and no external power supply is necessary to maintain the stored information. Nowadays, the NVM market is dominated by the silicon-based Flash. However, there are a few drawbacks for Flash, including scaling issue, relatively slow operation speed, and high voltage for program/erase operations [2]. Even though the three-dimensional crossbar structure may solve the low-density issue of Flash temporarily [3], the market demands next-generation NVM that has overall advantages over Flash. In general, next-generation NVM should exhibit outstanding properties including high density, excellent scalability, low power consumption, and low cost. Resistive random access memory (RRAM) is one of the promising candidates that fulfill the requirements of next-generation NVM. Additionally, RRAM has simple metal/insulator/metal sandwich structure (Fig. 1(a)) [4] and good complementary metal-oxide-semiconductor (CMOS) compatibility, which are vital for its practical applications and mass productions. As implied by the name, RRAM is the memory using the switch of resistance under electric field to record information, where the high and low resistance states correspond to the logic 0 and 1, respectively. The key component of the memory is the insulating resistance switch (RS) layer, as shown in Fig. 1(a), while it should be pointed out that in some cases the top/bottom electrodes can also be involved in the RS process. In RRAM, the transition from high resistance state (HRS) to low resistance state (LRS) is normally called "set", while the reversed transition is named "reset". Two switching modes exist in RRAM, unipolar and bipolar; for unipolar mode, the switching is independent on the polarity of the applied voltage, while for

* Corresponding author. School of Materials Science and Engineering, Beihang University, Beijing 100191, China.
*E-mail address:* zmsun@buaa.edu.cn (Z. Sun).
Peer review under responsibility of The Chinese Ceramic Society.

http://dx.doi.org/10.1016/j.jmat.2015.07.009

bipolar switching, opposite polarity of voltage is required, as shown in Fig. 1(b).

The academic and industrial research topics on RRAM cover quite a wide range: materials problem, RS mechanism, manufacture, integration, and even other function beyond the data storage, as reviewed previously [1–15]. In this review article, we concentrate on the materials science issue including the material selection and the corresponding RS mechanisms. To avoid the overlapping with other previous reviews, we mainly focus on the very latest research results. Also the promising role of computational materials science in the design of new RRAM is highlighted here. Correspondingly, the structure of this paper is organized as follows: first, some general hints for materials selection for RRAM; second, the materials that have been investigated for RRAM are summarized; third, the RS mechanisms are shown; finally, the importance of computational materials science for the development of RRAM is discussed.

## 2. Some hints for materials selection for RRAM

As for a specific material, the high and low resistance state (logic 0 and 1) should correspond to its two structures that are different at least in the electronic/atomic or even nano-/micro-scale. The two structures, denoted as Struc.0 and Struc.1 in Fig. 2, may have different energy. In essence, the resistance switch is simply a transition between two structures (or two phases, in some cases) of the material in the presence of electric field, while the striking feature for RRAM application compared to normal phase transition is that the involved two structures should have distinct resistance contrast. The structural transition (resistance switch) process is illustrated in Fig. 2. As an appropriate materials for RRAM, the values of "D", "$E_{set}$", "$E_{reset}$", "$E_{diff}$" and "R" should be quite small, which can lead to the high endurance, low power consumption and high operation speed of the device. However, the too small "$E_{set}$" and "$E_{reset}$" may impair the retention of the memory. Here, we tried to present a clear connection between performance of the device and the property of the material, and make it easier for the material scientists to participate in the optimization of RRAM. However, it should be noticed that these parameters are actually correlated and not totally independent, for example, a large "$E_{diff}$" may mean that "$E_{set}$" is much smaller than "$E_{reset}$". Anyway, Fig. 2 should provide very general hints to find advanced materials for RRAM, and these hints may strengthen the potential contribution of computation materials science as will be discussed later.

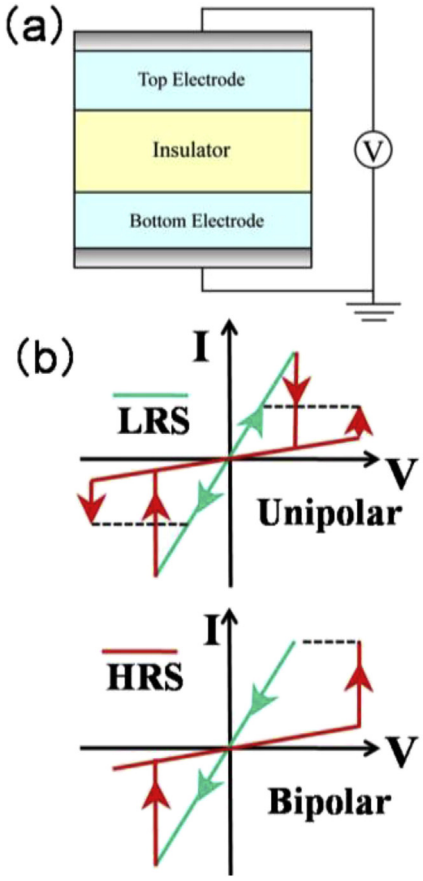


Fig. 1. (a) Sandwich structure of RRAM devices, top/bottom electrodes are normally metals, (b) Typical I–V curve of unipolar and bipolar switching modes.

## 3. Materials database

The first experimental observation of RS can be dated back to more than half a century ago. In 1962, Hickmott [16] found a large negative resistance in the current–voltage characteristics of five oxide films including $SiO_x$, $Al_2O_3$, $Ta_2O_5$, $ZrO_2$ and $TiO_2$. The urgency to find the replacement of Flash memory boosts the searching for RS phenomena in other materials, especially in the past few decades. A large variety of materials have been found exhibiting the RS behavior, which can be categorized into binary oxides, ternary and more complex

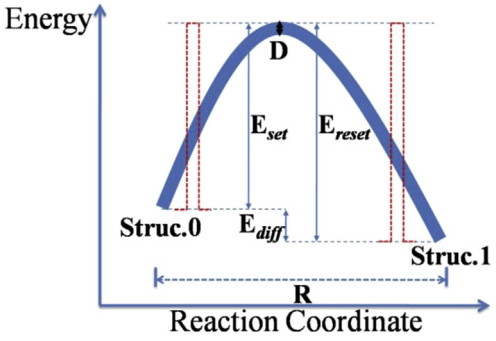


Fig. 2. Illustration of the energy profile of the transition between two structures of the material, as an analogy to the RS process in RRAM. The red column represents the energy needed can be supplied by the electric pulse. Parameter "D" means the reproducibility/stability of the transition path, corresponding to the endurance, uniformity and reliability of RRAM; "$E_{set}$" is the overall energy needed for Struc.0 to Struc.1 transition, corresponding to voltage and power needed for set process; "$E_{reset}$" is the overall energy needed for Struc.1 to Struc.0 transition, corresponding to the voltage and power needed for reset process; "$E_{set}$" and "$E_{reset}$" are also related to the retention of RRAM; "$E_{diff}$" is the energy difference of the two states, corresponding to the relative retention of the devices; "R" (reaction coordinate) is the displacements of any electrons/ions involved in the RS process, corresponding to the operation time.

oxides, chalcogenides, nitrides, amorphous-silicon/carbon, and some organic materials with specific application in flexible electronic devices. The switching performance of these materials, such as switching mode, operation speed, endurance, etc, has been well summarized in previous reviews [1–14].

Among the materials with RS behavior, binary oxides have been extensively investigated due to its relatively easy fabrication process and satisfying stability. Here, to give a general clue of the composition of these binary oxides, a periodic table is shown below in Fig. 3, and the host metallic elements of these oxides studied as RS materials are highlighted. The nominal valence state of these metallic elements, the microstructures of the oxides (crystalline or amorphous), and whether the electrodes are directly involved in the RS process are also indicated in the figure. As can be seen from the figure, some binary oxides have been studied quite thoroughly, such as the Ta–O systems, while others have not attracted many attentions yet, leaving more room for future research. It is worth noting that RS layers can be heterostructures consisting of more than one oxide, adding more degrees of freedom for material selection.

## 4. Resistance switch mechanisms

So far, a few mechanisms have been proposed to explain the RS phenomena, each of which accounts for the RS behavior of a series of materials, as can be found from previous reviews. As mentioned in Section 2, the RS process is similar to the structure/phase transition in materials science. The structure/phase transition is normally related to various defects, which can be divided into point, linear, or planer defects according to the length scale. By analogy, we roughly re-classify those RS mechanisms into a few groups based on their "scale": carrier trapping/de-trapping (electronic scale), migration of point defect (atomic scale), metal-insulator-transition (apparent change of the atomic structure), thermochemical reaction (apparent change of the microstructure), and complex mechanism. The changes of the resistance due to various mechanisms are actually caused by the evolution of these defected structures triggered by the electric/thermal effects, a typical structure-property relation in materials science. In the following part, the definitions of these mechanisms including some of their combinations will be briefly introduced, and the newly reported materials that fall into respective categories will be mentioned.

### 4.1. Carrier trapping/de-trapping

The charge carrier can be trapped by the defects inside the insulator layer or by the electrode/insulator interface, which will build an internal electric filed and impact the injection or transport of the carrier that eventually leads to the RS behavior.

Space-charge-limited conduction (SCLC) takes place when the charge is trapped by the point defects such as the vacancies inside the insulator layer. This effect brings the bipolar switching where the trapping and de-trapping corresponds to applied voltage with opposite polarity.

When a Schottky barrier is formed on the electrode/insulator interface, carries can be trapped, which in turn change the

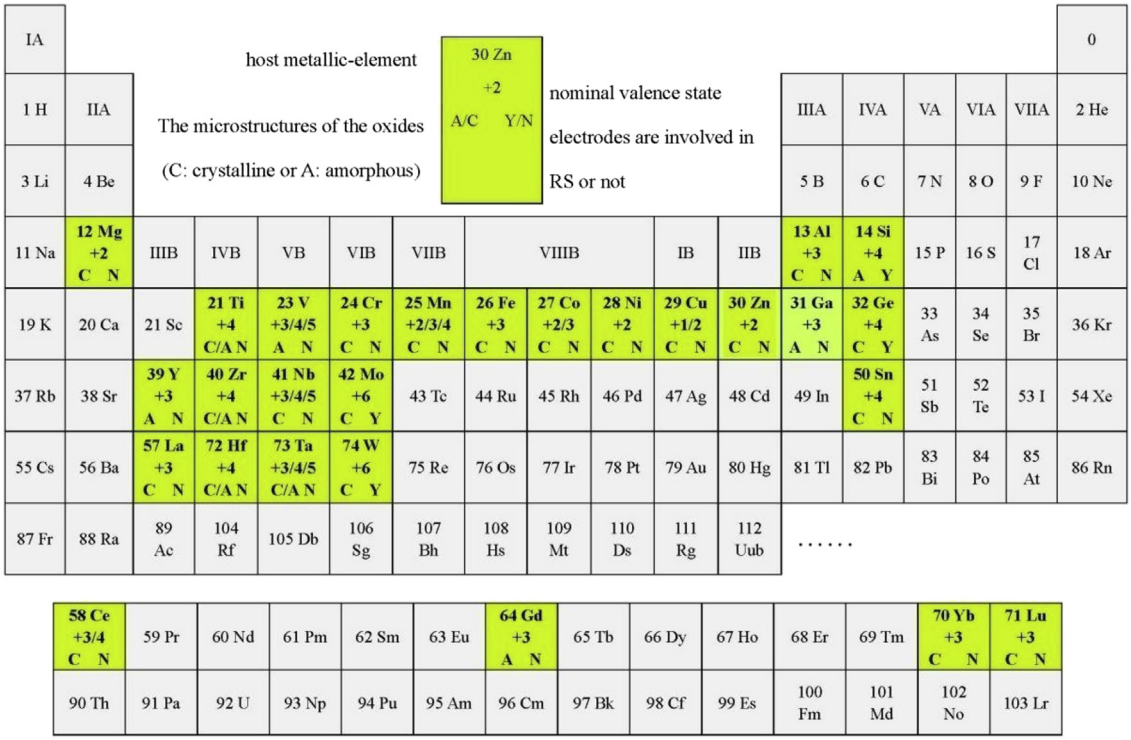


Fig. 3. Periodic Table with the host metal of RRAM used oxides highlighted. The details of these RRAM devices can be found in recently published work (Ref. [17–49]) and references therein.

height of barrier and affect the transport of the charges. The external voltage applied can modulate the Schottky barrier height and results in the RS behavior.

Generally, switching process occurs at the electronic scale should be faster, indicating a shorter write time, and considering the parameters in Fig. 2, the value of "R" should be very small. However, good retention can not be assured meanwhile, as shown in the voltage-time dilemma by Schroeder et al. [50].

### 4.2. Migration of point defects

In fact, migration of point defects can be involved in various mechanisms, including those in the following two sections, while the difference here is the migration of defects playing a dominant role. For the oxides, the formation and migration of anions/cations inevitably cause the valence-state change of the cations/anions. Regarding this, point-defects migration based RRAM are also called valence change memory (VCM). Normally, RRAM with this mechanism has a bipolar feature as a result of the huge effects of external electric field on the migration of charged defects.

To obtain a big change of the resistance, massive point defects should be formed or clustered, and their clustering usually generates a conduction path called filament. Filamentary conduction mechanism has been confirmed in many RRAM. Very recently, Shang et al. [51] reported a transparent RRAM based on all-oxide heterostructure indium-tin oxide/hafnium oxide/indium-tin oxide (ITO/$HfO_x$/ITO), showing asymmetric bipolar RS behavior. The mechanism is found to be the electric field induced migration of oxygen anions and the simultaneous formation of Hf-rich filament. This transparent RRAM is initial electroforming free, since the $HfO_x$ layer was fabricated at the oxygen poor condition with an $O_2$/Ar ratio of 1:5, leaving numerous oxygen vacancies inside the oxides at the first stage. The experimental clue of the proposed RS mechanism is shown in Fig. 4. Here one ITO electrode is replaced by inert metal Pt to avoid bringing extra atoms from ITO into the film upon argon etching treatments. As this RRAM is forming-free, the initial resistance state (IRS) is the similar as the high resistance state (HRS) normally referred to. As shown in Fig. 4, during the switch from IRS to LRS the change of oxygen content is significant, suggesting its domination on the RS behavior, while the change of the Hf-ions content is less apparent [51].

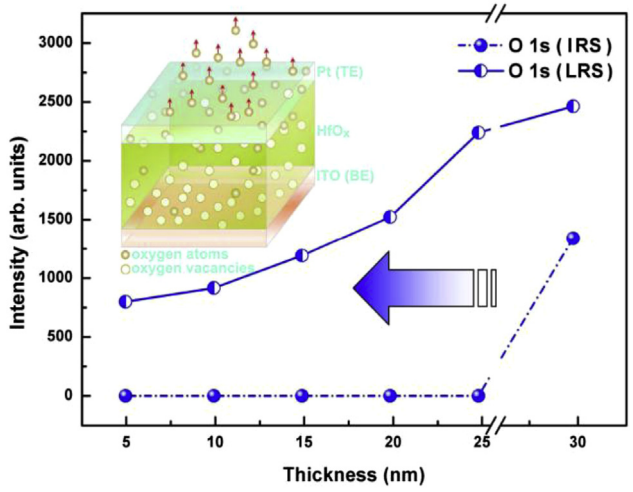


Fig. 4. IRS and LRS distribution of the oxygen content in the Pt electrode layer of the Pt/$HfO_x$/ITO structure. Position of Pt/$HfO_x$ interface is near the thickness of 25 nm. The inset is a schematic illustration of the migration of oxygen anions towards the metal electrode. Reprinted with permission from Ref. [51]. Copyright 2013 WILEY-VCH.

$TiO_2$ has been extensively explored as the RS material, depending on its microstructure (polycrystalline or amorphous), different mechanisms have been reported, including the redox interaction mechanism shown in Section 4.4. Lately, Hu et al. [52] fabricated a RRAM based on the single-crystalline anatase $TiO_2$, with the RS mechanism proposed to be the filament type. Fig. 5 illustrates that the diffusion of oxygen vacancy accounts for the resistance switch. However, it is noteworthy that even the diffusion of oxygen vacancy takes control, the authors did not rule out the contribution of the local phase transformation to Magnéli phase as is discussed in Section 4.4.

### 4.3. Metal-insulator-transition (MIT)

Materials with MIT behavior is naturally a promising RS material, given the distinct conductivity change after the transition. The work left is to figure out whether this MIT is easily controllable. Dioxide of group VB elements $VO_2$ [53] and $NbO_2$ [54] exhibit MIT, as well as $Ca_2RuO_4$ [55]. Fig. 6 shows one phase diagram of $VO_2$. $VO_2$ can exist in three different structures depending on the temperature and strain, including two insulating (M1 and M2) and one metallic rutile (R) phases, and triple point in the phase diagram was measured and confirmed by Park et al. [56], as shown in Fig. 6. It can be seen that phase transition can be realized by increasing/decreasing the environmental temperature and/or applied strain. MIT can also be driven by electric field induced Joule heating effect. However, regarding the quite lower temperature for the MIT, long time stability of different phases is doubtful, i.e., MIT of $VO_2$ can hardly reach the requirements of non-volatility. Also it has been proved that in the presence of external electric field, the formation of oxygen vacancy can suppress the MIT of $VO_2$ [57], which may further hinder its application.

So far, there is no experimental report about the MIT in $TaO_2$, although its counterparts in group VB ($VO_2$ and $NbO_2$) were reported. Recently, using evolution algorithm in combination with first-principles calculation, we found an insulating structure of $TaO_2$, and the MIT was theoretically predicted. The detail is introduced in Section 5.1.

The MIT mentioned above is a typical first-order phase transition, i.e., the microstructure of the phase or at least the atomic structure will be changed. There is also MIT belongs to the electronic scale process, such as a family of compounds $AM_4X_8$ Mott insulator (A = Ga, Ge; M = V, Nb; X = S, Se) [58]. These compounds exhibit a very small band gap of 0.2 ± 0.1 eV, indicating the high sensitivity to external perturbation, such as the pressure and electric field. Dobust

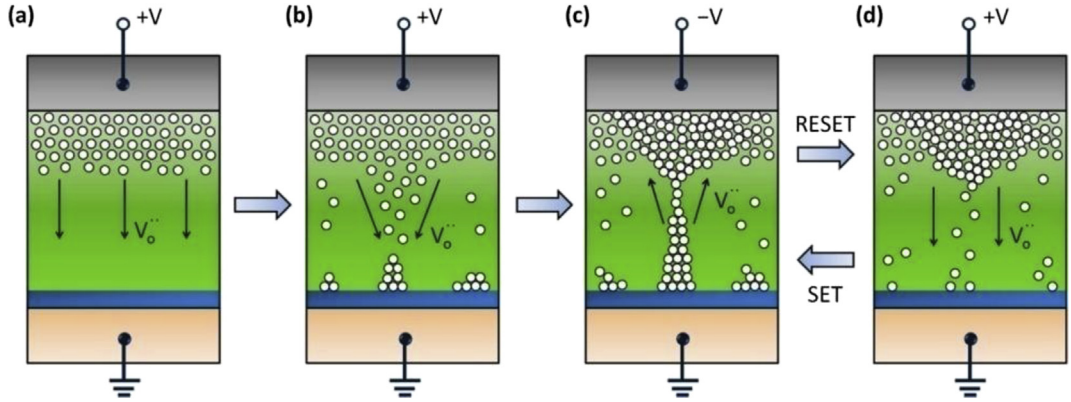


Fig. 5. Illustration of the proposed RS mechanism based on the I–V characteristics. In each part of the illustration, voltage is applied to the top contact after the depicted oxygen vacancy configuration is achieved within the $TiO_2$ matrix, and the arrows denote moving direction of oxygen vacancies upon application of voltage to the top contact. Oxygen vacancy configuration (a) in the pristine state, (b) during the SET process, (c) in the ON state, and (d) in the OFF state. Reprinted with permission from Ref. [52]. Copyright 2014 American Chemical Society.

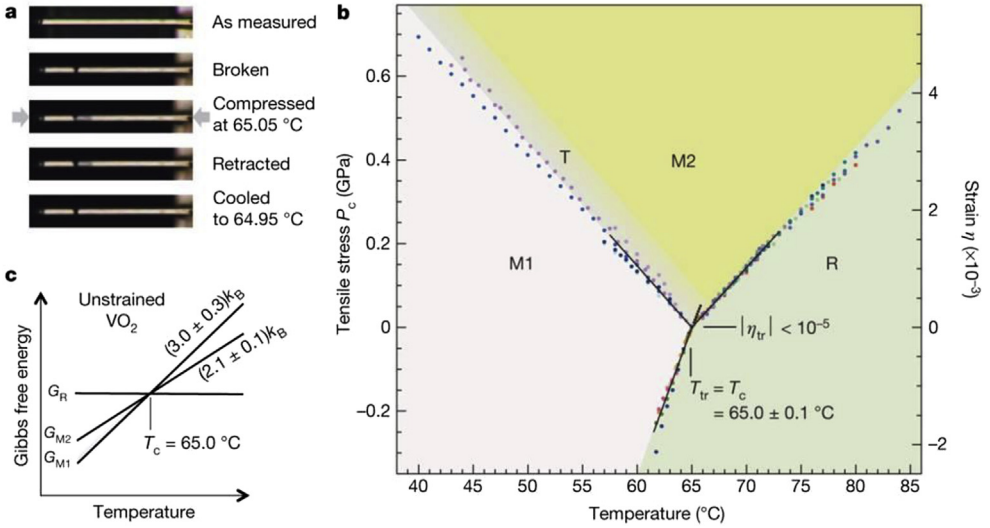


Fig. 6. Phase diagram of $VO_2$. a, The transition temperature $T_c$ at zero stress is measured by finding the temperature above which the metallic phase (darker) becomes stable in a cantilever. It is found to be equal to the triple point temperature: $T_c = T_{tr} = 65.0 \pm 0.1$ °C. b, Deduced stress–temperature phase diagram. The small black filled circles are for the superheated M1 phase. The grey shaded strip is where a metastable T phase (intermediate between M1 and M2) can occur. c, The results imply that the free energies of all the phases are degenerate at $T_c$ in unstrained pure $VO_2$. Reprinted with permission from Ref. [56]. Copyright 2013 Macmillan Publishers Limited.

et al. [59] ascribed the transition to the appearance of metallic and super-insulating nano-domains and strong electron-lattice coupling by means of scanning tunneling microscopy/spectroscopy (STM/STS). They also found that the MIT can even be triggered by the electric field of a STM tip.

### 4.4. Thermochemical reaction

Electric field can cause Joule heating, which may provide the temperature condition required by any possible chemical reaction in the RRAM device. The RS caused by this mechanism is normally unipolar, due to the fact that generation of heat is independent on the polarity of the electric field. Since the oxides formed by one single metallic element are abundant, as indicated by the Ellingham diagram, the different electronic property of these oxides may induce the RS phenomena. Again, taking RRAM based on $TiO_2$ as the example, the conducting $Ti_nO_{2n-1}$(n = 3–5 for rutile and 5–7 for anatase) Magnéli phase can be formed [60] after the thermochemical reaction, with contrast resistance compared to insulation rutile $TiO_2$. In practice, this chemical reaction does not take place in the whole device; instead, a filament-type conductive product is enough to short-circuit the device. Many oxide based RRAM have this mechanism for RS, such as NiO, CoO, $Nb_2O_5$, etc, as summarized in Ref. [12].

### 4.5. Complex mechanism

The complexity of RS mechanism not only comes from its variety but also from the correlation between different

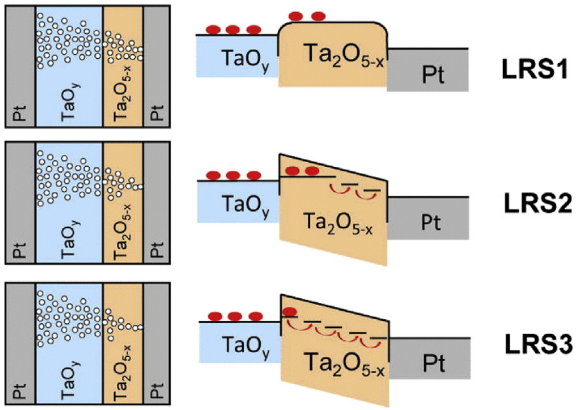


Fig. 7. Possible conduction mechanism for three different LRS. Reprinted with permission from Ref. [63]. Copyright 2014 AIP Publishing LLC.

mechanisms [61,62]. Zhang et al. [63] reported the coexistence of metallic and hopping conduction at the low resistance state (LRS) of $Ta_2O_{5-x}/TaO_y$ based RRAM, and three types of conduction behaviors were found by temperature-dependent measurements ranging from 5 K to 250 K. The LRS was divided into three stages, denoted by LRS1, LRS2 and LRS3, respectively, as shown in Fig. 7. At LRS1 (very low resistance), metallic conduction is dominated due to the formation of metallic filament, while at LRS3 electrons hopping between localized states has more contribution and LRS2 is the transition process. When temperature goes down, the metallic conduction transfers to the electrons hopping which was observed clearly at temperature below 20 K, with the phenomenon that a positive temperature dependence of resistance transfers to a negative one.

## 5. Future prospects: opportunity of computational materials science

As shown above, the complexity and variety of the RS mechanism bring many challenges for the design of advanced RRAM. With the rapid development of computer technology and computation algorithms, computational materials science has been placed at a very important position for the design of new materials. As the materials used in RRAM devices come to the nano-scale and even single-crystalline stage, accurate and solid calculations based on first-principles method and (ab initio) molecular dynamics will become powerful tools for the design of RRAM devices. In the following sections, we will show some latest results in this scope.

### 5.1. Prediction of new materials

In this section, the "new" materials represent the materials with stoichimetry and/or symmetry that are different from the

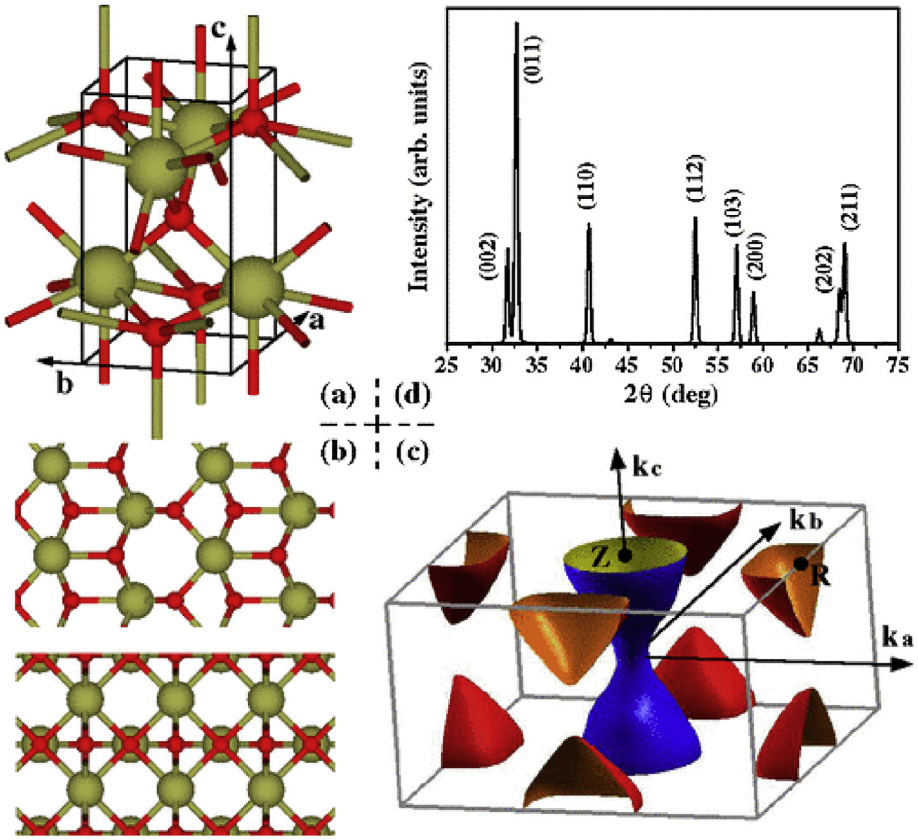


Fig. 8. Tetragonal $Hf_2O_3$ and $Zr_2O_3$. (a) Primitive cell with 5 atoms, (b) view along *a* axis (upper) and *c* axis (lower), (c) Fermi surface of $Hf_2O_3$ at T = 0 K, (d) simulated powder x-ray diffraction patterns of $Hf_2O_3$. Big green balls, Hf or Zr; small red balls, O. Reprinted with permission from Ref. [64]. Copyright 2013 American Physical Society.

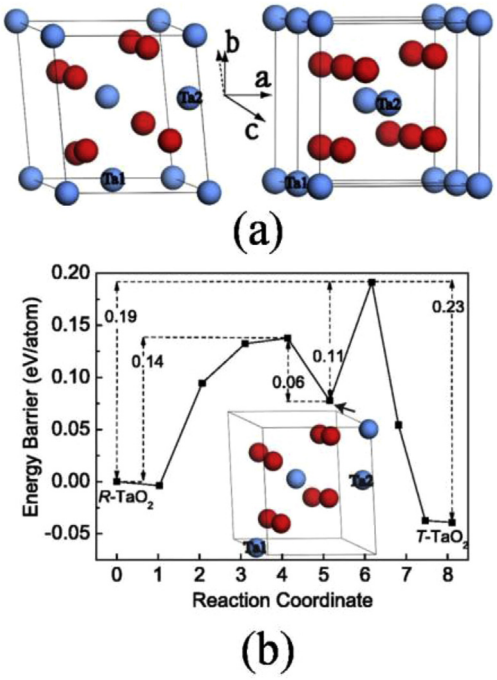


Fig. 9. (a) Left: Unit cell of triclinic $TaO_2$. Right: $1 \times 1 \times 2$ supercell of rutile $TaO_2$. Blue and red balls represent Ta and O, respectively, and the two (super) structures shown here have the same number of atoms. Ta atoms showing the most significant displacements in the two structures are labeled as Ta1 and Ta2. (b) Transition path from $R$—$TaO_2$ to $T$—$TaO_2$, the energy difference between various states is labeled in the unit of eV/atom. Structure of the metastable intermediate state as denoted by the solid arrow is also shown. Reprinted with permission from Ref. [65]. Copyright 2015 AIP Publishing LLC.

established database. $Ti_nO_{2n-1}$ Magnéli phase was found responsible for the LRS of $TiO_2$ based RRAM. It is very likely that similar oxygen-deficient phases exist in RRAM based on some other transition metal oxide, even there are not many experimental results reported yet. Xue et al. [64] predicted a

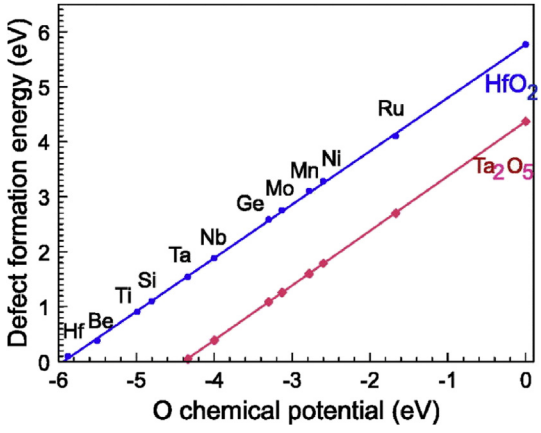


Fig. 10. Variation of O vacancy formation energy with local $\mu_O$ for $HfO_2$ and $Ta_2O_5$ as examples. The scavenging metal (shown) can be used to set $\mu_O$ and thus control the $V_O$ formation energy and $V_O$ concentration independently of the host oxide. This allows independent optimization of some device performance parameters. Reprinted with permission from Ref. [71]. Copyright 2014 AIP Publishing LLC.

semimetallic tetragonal $Hf_2O_3$ and $Zr_2O_3$ by using the first-principles calculations. The new structures of the oxides are shown in Fig. 8, together with the simulated XRD pattern that might be helpful for further experimental confirmation. The overlap of the partially filled valence band top and conduction band bottom at the different high symmetry points in the Brillouin zone was found by $G_0W_0$ calculations with the many-body correction to the GGA energy levels, indicating the semimetallic feature of these oxides. The oxides have an estimated carrier concentration of $1.8 \times 10^{21}$ $cm^{-3}$ for both electrons and holes, and this electric conduction may explain the LRS of RRAM based on hafnia and zirconia.

Recently, we did a thorough structure searching using evolution algorithm, and found a stable triclinic phase of $TaO_2$ which is more stable than its rutile counterpart [65]. Based on the electronic structure calculations, $TaO_2$ was demonstrated to have the MIT behavior induced by the Peierls distortion. The atomic structure of the rutile phase ($R$—$TaO_2$, metallic phase) and the predicted triclinic phase ($T$-$TaO_2$, insulator) are shown in Fig. 9(a). The transition path between these two phases was figured out based on the calculation using transition state theory (Fig. 9(b)), and the energy barrier for the reversible transition is 0.19 eV/atom and 0.23 eV/atom, respectively, suggesting lower power consumption for the RS. Interestingly, the MIT should be driven by the electric field, since the transition is triggered by the directional displacements of only two Ta ions (12 atoms in total in the unit cell), which makes it a promising bipolar-RRAM material.

In fact, structure prediction based on the first-principles calculation in combination with approaches such as evolution algorithm is a very mature technique in computational materials science. Very fruitful works have been reported using the structure-prediction codes such as USPEX [66,67], CALYPSO [68,69] and AIRSS [70] in the past decade. These techniques should be very helpful to figure out any possible and undiscovered (meta-) stable phases generated during the RS process, which can give more insights into the RS behavior.

### 5.2. Material screening by first-principles calculation

Since the behavior of the point defects in the RS material has substantial effects on the performance of RRAM, the time-saving theoretical calculations on this topic should give valuable information to the device designer when they select the RS materials needed.

Guo et al. [71] investigated the energy of the RS process for typical oxides, including the formation energy and diffusion barrier of oxygen vacancy (Vo). Fig. 10 shows the formation energy of oxygen vacancy as the function of oxygen chemical potential ($\mu_O$) in $HfO_2$ and $Ta_2O_5$. The idea here is using a scavenging layer located between the electrode and oxides to change the formation energy of oxygen vacancy via tuning the oxygen chemical potential. The scavenging layer can be made of metals as listed in Fig. 10. This result is meaningful when one wants more/less oxygen vacancy generated to optimize the performance of RRAM.

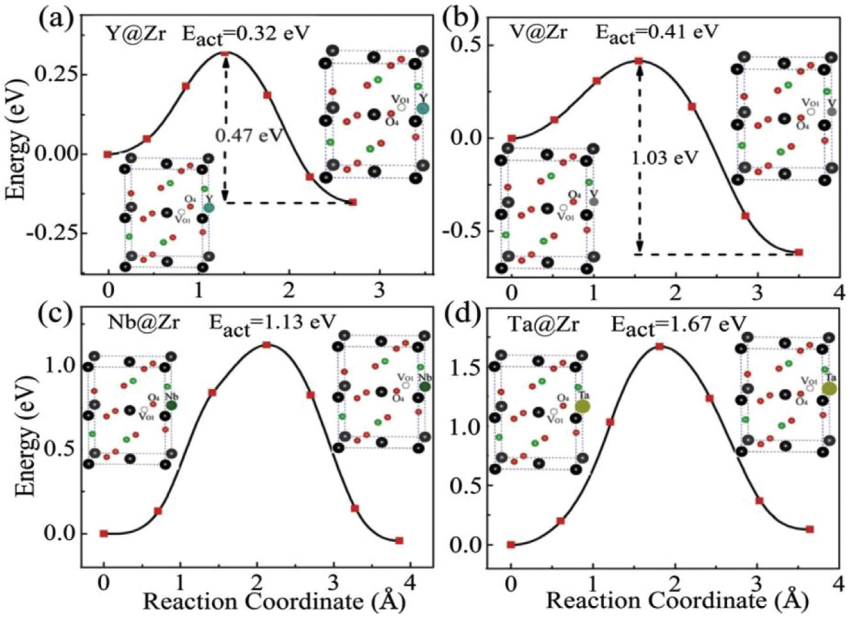


Fig. 11. The diffusion barrier curves of $V_o^{2+}$ in (a) Y-doped, (b) V-doped, (c) Nb-doped and (d) Ta-doped SZO systems. Here only the diffusion profiles on the most probable path are shown. The insets are the atomic structures of the doped SZO. Reproduced by permission of the Royal Society of Chemistry from Ref. [74].

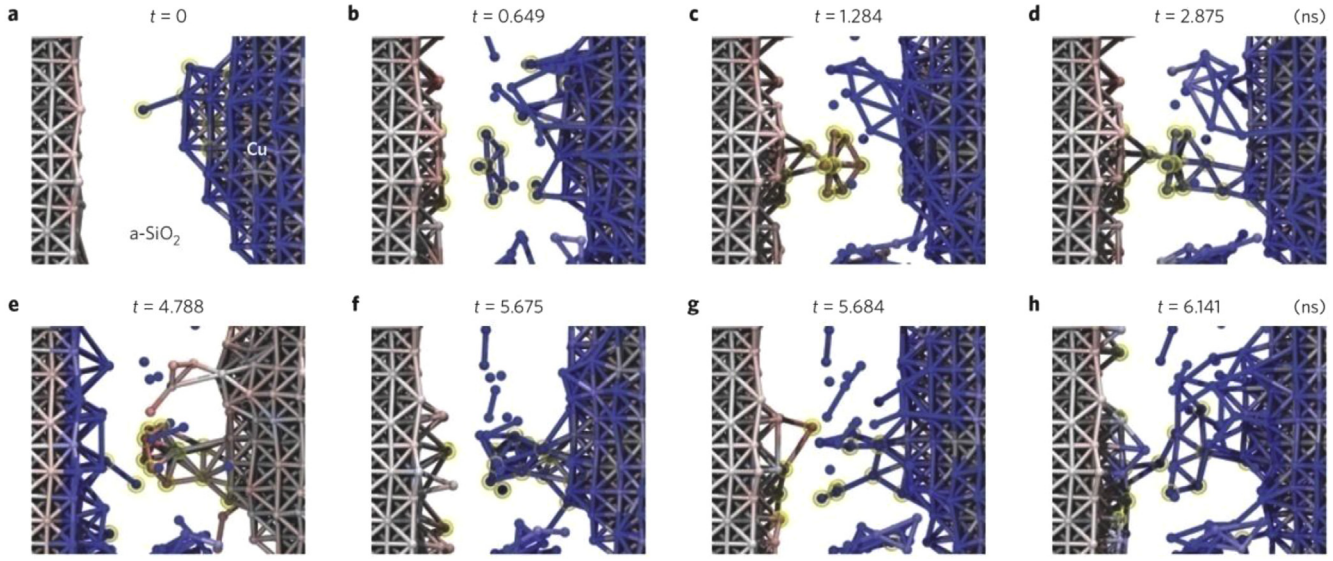


Fig. 12. Atomic mechanisms of filament formation and dissolution. a–h, Snapshots zooming in at the filament during the forming/reset/set phases. The yellow spheres follow the constituent atoms of the first filament established during the forming phase (d). In all snapshots, color represents atomic charges, ranging from red (−0.3e) to blue (+0.3e), and amorphous $SiO_2$ has been hidden for clarity. Reprinted with permission from Ref. [75]. Copyright 2015 Macmillan Publishers Limited.

Ternary oxide $SrZrO_3$ (SZO) has been used as RS material, and the conductive filament was believed to be formed by oxygen vacancies [72]. Previously, our first-principles calculations [73] provided a solid proof for the important role of oxygen vacancy. We found that formation of oxygen vacancy row results in the defect assisted conduction channel, corresponding to the LRS of RRAM, while the disruption of this ordered vacancy row breaks the conduction channel resulting in the HRS. Doping is an effective method to optimize the properties of the RS material and the performance of RRAM. Lately, we did a systemic investigation on doping effects on the diffusion of oxygen vacancy in the matrix SZO [74]. The diffusion barrier of oxygen vacancy with change state of 2+ in doped SZO can be found in Fig. 11. For pristine SZO, the energy curve is parabolic with a barrier of 0.65 eV. It can be seen from Fig. 11 that doping has quite apparent effects on the diffusion of oxygen vacancy in terms of the diffusion-curve shape and energy barrier. Among various elements the impacts of Y and V are more significant. We also found that the influence of the dopant is related to its valence electron number and atomic radius, providing some general guidelines for designing related RRAM.

### 5.3. Simulation of the working device

In Sections 5.1 and 5.2, we showed the information that can be provided using first-principles calculations, a parameter-free and extremely accurate method. However, this information is sort of "stationary", while obviously the RS process is dynamic. For advanced nanoscale RRAM devices with ultra-fast RS speed, molecular dynamics might be a feasible tool to simulate the RS process considering the length and time scale of this method. Encouragingly, Onofrio et al. [75] reported the first atomic simulation of filament formation/rupture process using reactive molecular dynamics with a charge equilibrium method extended to describe electrochemical reactions in Cu/amorphous-silica based RRAM. The detailed RS process at the atomic scale can be seen in Fig. 12, in which the active Cu electrode plays a critical role in the filament formation. They found that single-atom-chain filaments can be formed in the RS process while they are metastable with lifetime less than a nanosecond, and formation of small metallic clusters due to the aggregation of ions is necessary for the occurrence of stable filament.

As claimed by the authors, simulation at this scale can basically capture all the possible process taking place in the operation of RRAM, such as electrochemical dissolution, ionic diffusion, nucleation and growth, all of which are significant for the optimization and design of RRAM devices.

In fact, the critical status of computational materials science in the design of NVM has already been demonstrated in the research of PCRAM (phase-change RAM), and other functional materials with electric-field induced phenomena, such as magnetoelectric heterostructures [76]. Both Ab initio [77–80] and Ab initio molecular dynamics simulations [81–83] generated very meaningful information for the design and understanding of PCRAM. There should be no doubt of its power here, in the design of RRAM.

## 6. Conclusion

In summary, the latest work on RRAM investigation especially in the field of materials science is reviewed. The materials with the RS behavior and the underlying mechanisms are briefly summarized. Compared to previous reviews, we emphasize the important role of computational materials science in the design of RRAM, which should have been proved in recent interesting work. It can be seen that the fundamental theories in materials science is very valuable for the design of RRAM and more material scientists should get involved into the research of this promising next-generation NVM.

## Acknowledgments

This work was partially supported by National Natural Science Foundation for Distinguished Young Scientists of China (No. 51225205), the National Natural Science Foundation of China (Nos. 61274005 and 37691801).

## References

[1] Han ST, Zhou Y, Roy VAL. Towards the development of flexible non-volatile memories. Adv Mater 2013;25:5425–49.
[2] Akinaga H, Shima H. ReRAM technology; challenges and prospects. IEICE Electron Express 2012;9:795–807.
[3] Seok JY, Song SJ, Yoon JH, Yoon KJ, Park TH, Kwon DE, et al. A review of three-dimensional resistive switching cross-bar array memories from the integration and materials property points of view. Adv Funct Mater 2014;24:5316–39.
[4] Akinaga H, Shima H. Resistive random access memory (ReRAM) based on metal oxides. Proc IEEE 2010;98:2237–51.
[5] Zhang M, Long S, Wang G, Li Y, Xu X, Liu H, et al. An overview of the switching parameter variation of RRAM. Chin Sci Bull 2014;59:5324–37.
[6] Pan F, Gao S, Chen C, Song C, Zeng F. Recent progress in resistive random access memories: materials, switching mechanisms, and performance. Mater Sci Eng R-Rep 2014;83:1–59.
[7] Yang JJ, Strukov DB, Stewart DR. Memristive devices for computing. Nat Nanotech 2013;8:13–24.
[8] Tian XZ, Wang LF, Li XM, Wei JK, Yang SZ, Xu Z, et al. Recent development of studies on the mechanism of resistive memories in several metal oxides. Sci China-Phys Mech Astron 2013;56:2361–9.
[9] Prakash A, Jana D, Maikap S. TaO(x) -based resistive switching memories: prospective and challenges. Nanoscale Res Lett 2013;8:418.
[10] Doo Seok J, Reji T, Katiyar RS, Scott JF, Kohlstedt H, Petraru A, et al. Emerging memories: resistive switching mechanisms and current status. Rep Prog Phys 2012;75:076502.
[11] Li Y, Long S, Liu Q, Lü H, Liu S, Liu M. An overview of resistive random access memory devices. Chin Sci Bull 2011;56:3072–8.
[12] Kyung Min K, Doo Seok J, Cheol Seong H. Nanofilamentary resistive switching in binary oxide system; a review on the present status and outlook. Nanotechnology 2011;22:254002.
[13] Cho B, Song S, Ji Y, Kim T-W, Lee T. Organic resistive memory devices: performance enhancement, integration, and advanced architectures. Adv Funct Mater 2011;21:2806–29.
[14] Waser R, Dittmann R, Staikov G, Szot K. Redox-based resistive switching memories – nanoionic mechanisms, prospects, and challenges. Adv Mater 2009;21:2632–63.
[15] Zhu X-J, Shang J, Li R-W. Resistive switching effects in oxide sandwiched structures. Front Mater Sci 2012;6:183–206.
[16] Hickmott TW. Low-Frequency negative resistance in thin anodic oxide films. J Appl Phys 1962;33:2669–82.
[17] Liang L, Li K, Xiao C, Fan S, Liu J, Zhang W, et al. Vacancy associates-rich ultrathin nanosheets for high performance and flexible nonvolatile memory device. J Am Chem Soc 2015;137:3102–8.
[18] Kim KM, Lee SR, Kim S, Chang M, Hwang CS. Self-limited switching in $Ta_2O_5$/TaOx memristors exhibiting uniform multilevel changes in resistance. Adv Funct Mater 2015;25:1527–34.
[19] Chen Z, Zhang FF, Chen B, Zheng Y, Gao B, Liu LF, et al. High-performance HfOx/AlOy-based resistive switching memory cross-point array fabricated by atomic layer deposition. Nanoscale Res Lett 2015;10:70.
[20] Chang K-C, Chang T-C, Tsai T-M, Zhang R, Hung Y-C, Syu Y-E, et al. Physical and chemical mechanisms in oxide-based resistance random access memory. Nanoscale Res Lett 2015;10:120.
[21] Chand U, Huang C-Y, Jieng J-H, Jang W-Y, Lin C-H, Tseng T-Y. Suppression of endurance degradation by utilizing oxygen plasma treatment in $HfO_2$ resistive switching memory. Appl Phys Lett 2015;106:153502.
[22] Zhou Q, Zhai J. Study of the bipolar resistive-switching behaviors in Pt/GdOx/TaNx structure for RRAM application. Phys Status Solidi A 2014;211:173–9.
[23] Yan XB, Hao H, Chen YF, Li YC, Banerjee W. Highly transparent bipolar resistive switching memory with In-Ga-Zn-O semiconducting electrode in In-Ga-Zn-O/$Ga_2O_3$/In-Ga-Zn-O structure. Appl Phys Lett 2014;105:093502.

[24] Sun H, Liu Q, Long S, Lv H, Banerjee W, Liu M. Multilevel unipolar resistive switching with negative differential resistance effect in Ag/$SiO_2$/Pt device. J Appl Phys 2014;116:154509–13.
[25] Nieh CH, Lu ML, Weng TM, Chen YF. Resistive memory of single $SnO_2$ nanowire based switchable diodes. Appl Phys Lett 2014;104:213501.
[26] Koza JA, Schroen IP, Willmering MM, Switzer JA. Electrochemical synthesis and nonvolatile resistance switching of $Mn_3O_4$ thin films. Chem Mater 2014;26:4425–32.
[27] Ji L, Chang Y-F, Fowler B, Chen Y-C, Tsai T-M, Chang K-C, et al. Integrated one Diode–One resistor architecture in nanopillar SiOx resistive switching memory by nanosphere lithography. Nano Lett 2014;14:813–8.
[28] Ismail M, Huang C-Y, Panda D, Hung C-J, Tsai T-L, Jieng J-H, et al. Forming-free bipolar resistive switching in nonstoichiometric ceria films. Nanoscale Res Lett 2014;9:1–8.
[29] Zhao H, Tu H, Wei F, Xiong Y, Zhang X, Du J. Characteristics and mechanism of nano-polycrystalline $La_2O_3$ thin-film resistance switching memory. Phys Status Solidi RRL 2013;7:1005–8.
[30] Zhang T, Yin J, Xia Y, Zhang W, Liu Z. Conduction mechanism of resistance switching in fully transparent MgO-based memory devices. J Appl Phys 2013;114:134301.
[31] Park G-S, Kim YB, Park SY, Li XS, Heo S, Lee M-J, et al. In situ observation of filamentary conducting channels in an asymmetric $Ta_2O_{5-x}/TaO_{2-x}$ bilayer structure. Nat Commun 2013;4:2382.
[32] Long S, Perniola L, Cagli C, Buckley J, Lian X, Miranda E, et al. Voltage and power-controlled regimes in the progressive unipolar RESET transition of $HfO_2$-based RRAM. Sci Rep 2013;3:2929.
[33] Kim J-D, Baek Y-J, Jin Choi Y, Jung Kang C, Ho Lee H, Kim H-M, et al. Investigation of analog memristive switching of iron oxide nanoparticle assembly between Pt electrodes. J Appl Phys 2013;114:224505.
[34] Chao X, Biao N, Long Z, Long-Hui Z, Yong-Qiang Y, Xian-He W, et al. High-performance nonvolatile Al/AlOx/CdTe:Sb nanowire memory device. Nanotechnology 2013;24:355203.
[35] Sadaf SM, Liu X, Son M, Park S, Choudhury SH, Cha E, et al. Highly uniform and reliable resistance switching properties in bilayer WOx/NbOx RRAM devices. Phys Status Solidi A 2012;209:1179–83.
[36] Rahaman SZ, Maikap S, Chen WS, Lee HY, Chen FT, Kao MJ, et al. Repeatable unipolar/bipolar resistive memory characteristics and switching mechanism using a Cu nanofilament in a GeOx film. Appl Phys Lett 2012;101:073106.
[37] Mondal S, Chen H-Y, Her J-L, Ko F-H, Pan T-M. Effect of Ti doping concentration on resistive switching behaviors of $Yb_2O_3$ memory cell. Appl Phys Lett 2012;101:083506.
[38] Huang Y-C, Chen P-Y, Chin T-S, Liu R-S, Huang C-Y, Lai C-H. Improvement of resistive switching in NiO-based nanowires by inserting Pt layers. Appl Phys Lett 2012;101:153106.
[39] Tohru T, Kazuya T, Tsuyoshi H, Masakazu A. Temperature effects on the switching kinetics of a Cu–$Ta_2O_5$ -based atomic switch. Nanotechnology 2011;22:254013.
[40] Pi C, Ren Y, Liu ZQ, Chim WK. Unipolar memristive switching in yttrium oxide and RESET current reduction using a yttrium interlayer. Electrochem Solid-State Lett 2011;15:G5–7.
[41] Lee M-J, Lee CB, Lee D, Lee SR, Chang M, Hur JH, et al. A fast, high-endurance and scalable non-volatile memory device made from asymmetric $Ta_2O_{5-x}/TaO_{2-x}$ bilayer structures. Nat Mater 2011;10:625–30.
[42] Chen S-C, Chang T-C, Chen S-Y, Chen C-W, Chen S-C, Sze SM, et al. Bipolar resistive switching of chromium oxide for resistive random access memory. Solid State Electron 2011;62:40–3.
[43] Gao X, Guo H, Xia Y, Yin J, Liu Z. Unipolar resistive switching characteristics in $Co_3O_4$ films. Thin Solid Films 2010;519:450–2.
[44] Yang MK, Park J-W, Ko TK, Lee J-K. Bipolar resistive switching behavior in Ti/$MnO_2$/Pt structure for nonvolatile memory devices. Appl Phys Lett 2009;95:042105.
[45] Shima H, Takano F, Muramatsu H, Akinaga H, Tamai Y, Inque IH, et al. Voltage polarity dependent low-power and high-speed resistance switching in CoO resistance random access memory with Ta electrode. Appl Phys Lett 2008;93:113504.
[46] Chen A, Haddad S, Wu YC, Fang TN, Kaza S, Lan Z. Erasing characteristics of $Cu_2O$ metal-insulator-metal resistive switching memory. Appl Phys Lett 2008;92:013503.
[47] Lee D, D-j Seong, Jo I, Xiang F, Dong R, Oh S, et al. Resistance switching of copper doped MoOx films for nonvolatile memory applications. Appl Phys Lett 2007;90:122104.
[48] Qin S, Zhang J, Fu D, Xie D, Wang Y, Qian H, et al. A physics/circuit-based switching model for carbon-based resistive memory with sp2/sp3 cluster conversion. Nanoscale 2012;4:6658–63.
[49] Hu B, Quhe R, Chen C, Zhuge F, Zhu X, Peng S, et al. Electrically controlled electron transfer and resistance switching in reduced graphene oxide noncovalently functionalized with thionine. J Mater Chem 2012;22:16422–30.
[50] Schroeder H, Zhirnov VV, Cavin RK, Waser R. Voltage-time dilemma of pure electronic mechanisms in resistive switching memory cells. J Appl Phys 2010;107:054517.
[51] Shang J, Liu G, Yang H, Zhu X, Chen X, Tan H, et al. Thermally stable transparent resistive random access memory based on all-oxide heterostructures. Adv Funct Mater 2014;24:2171–9.
[52] Hu C, McDaniel MD, Posadas A, Demkov AA, Ekerdt JG, Yu ET, et al. Highly controllable and stable quantized conductance and resistive switching mechanism in single-crystal $TiO_2$ resistive memory on silicon. Nano Lett 2014;14:4360–7.
[53] Kim J, Ko C, Frenzel A, Ramanathan S, Hoffman JE. Nanoscale imaging and control of resistance switching in $VO_2$ at room temperature. Appl Phys Lett 2010;96:213106.
[54] Xinjun L, Sharif Md S, Myungwoo S, Jungho S, Jubong P, Joonmyoung L, et al. Diode-less bilayer oxide (WOx–NbOx ) device for cross-point resistive memory applications. Nanotechnology 2011;22:475702.
[55] Nakamura F, Sakaki M, Yamanaka Y, Tamaru S, Suzuki T, Maeno Y. Electric-field-induced metal maintained by current of the Mott insulator $Ca_2RuO_4$. Sci Rep 2013;3:2536.
[56] Park JH, Coy JM, Kasirga TS, Huang C, Fei Z, Hunter S, et al. Measurement of a solid-state triple point at the metal-insulator transition in $VO_2$. Nature 2013;500:431–4.
[57] Jeong J, Aetukuri N, Graf T, Schladt TD, Samant MG, Parkin SSP. Suppression of metal-insulator transition in $VO_2$ by Electric Field–Induced oxygen vacancy formation. Science 2013;339:1402–5.
[58] Cario L, Vaju C, Corraze B, Guiot V, Janod E. Electric-field-induced resistive switching in a family of Mott insulators: towards a new Class of RRAM memories. Adv Mater 2010;22:5193–7.
[59] Dubost V, Cren T, Vaju C, Cario L, Corraze B, Janod E, et al. Resistive switching at the nanoscale in the Mott insulator compound $GaTa_4Se_8$. Nano Lett 2013;13:3648–53.
[60] Choi BJ, Jeong DS, Kim SK, Rohde C, Choi S, Oh JH, et al. Resistive switching mechanism of $TiO_2$ thin films grown by atomic-layer deposition. J Appl Phys 2005;98:033715.
[61] Gao S, Zeng F, Wang M, Wang G, Song C, Pan F. Tuning the switching behavior of binary oxide-based resistive memory devices by inserting an ultra-thin chemically active metal nanolayer: a case study on the $Ta_2O_5$-Ta system. Phys Chem Chem Phys 2015;17:12849–56.
[62] Yang YC, Chen C, Zeng F, Pan F. Multilevel resistance switching in Cu/TaOx/Pt structures induced by a coupled mechanism. J Appl Phys 2010;107:093701.
[63] Zhang Y, Deng N, Wu H, Yu Z, Zhang J, Qian H. Metallic to hopping conduction transition in $Ta_2O_{5-x}/TaO_y$ resistive switching device. Appl Phys Lett 2014;105:063508.
[64] Xue KH, Blaise P, Fonseca LRC, Nishi Y. Prediction of semimetallic tetragonal $Hf_2O_3$ and $Zr_2O_3$ from first principles. Phys Rev Lett 2013;110:065502.
[65] Zhu L, Zhou J, Guo Z, Sun Z. Realization of a reversible switching in $TaO_2$ polymorphs via Peierls distortion for resistance random access memory. Appl Phys Lett 2015;106:091903.
[66] Oganov AR, Lyakhov AO, Valle M. How evolutionary crystal structure prediction works—and why. Acc Chem Res 2011;44:227–37.

[67] Oganov AR, Glass CW. Crystal structure prediction using ab initio evolutionary techniques: principles and applications. J Chem Phys 2006;124:244704.
[68] Wang Y, Lv J, Zhu L, Ma Y. Crystal structure prediction via particle-swarm optimization. Phys Rev B 2010;82:094116.
[69] Wang Y, Lv J, Zhu L, Ma Y. CALYPSO: a method for crystal structure prediction. Comput Phys Commun 2012;183:2063–70.
[70] Chris JP, Needs RJ. Ab initio random structure searching. J Phys Condens Matter 2011;23:053201.
[71] Guo Y, Robertson J. Materials selection for oxide-based resistive random access memories. Appl Phys Lett 2014;105:223516.
[72] Wu J, Wen Z, Wu D, Zhai H, Li A. Current–voltage characteristics of sol–gel derived $SrZrO_3$ thin films for resistive memory applications. J Alloys Compd 2011;509:2050–3.
[73] Guo Z, Sa B, Zhou J, Sun Z. Role of oxygen vacancies in the resistive switching of $SrZrO_3$ for resistance random access memory. J Alloys Compd 2013;580:148–51.
[74] Guo Z, Zhu L, Zhou J, Sun Z. Design principles of tuning oxygen vacancy diffusion in $SrZrO_3$ for resistance random access memory. J Mater Chem C 2015;3:4081–5.
[75] Onofrio N, Guzman D, Strachan A. Atomic origin of ultrafast resistance switching in nanoscale electrometallization cells. Nat Mater 2015;14:440–6.
[76] Martin LW, Ramesh R. Multiferroic and magnetoelectric heterostructures. Acta Mater 2012;60:2449–70.
[77] Sun Z, Zhou J, Blomqvist A, Johansson B, Ahuja R. Formation of large voids in the amorphous phase-change memory $Ge_2Sb_2Te_5$ Alloy. Phys Rev Lett 2009;102:075504.
[78] Sun Z, Zhou J, Ahuja R. Unique melting behavior in phase-change materials for rewritable data storage. Phys Rev Lett 2007;98:055505.
[79] Sun Z, Zhou J, Ahuja R. Structure of phase change materials for data storage. Phys Rev Lett 2006;96:055507–10.
[80] Deringer VL, Dronskowski R. DFT studies of pristine hexagonal $Ge_1Sb_2Te_4$(0001), $Ge_2Sb_2Te_5$(0001), and $Ge_1Sb_4Te_7$(0001) surfaces. J Phys Chem C 2013;117:15075–89.
[81] Zhang W, Ronneberger I, Zalden P, Xu M, Salinga M, Wuttig M, et al. How fragility makes phase-change data storage robust: insights from ab initio simulations. Sci Rep 2014;4:6529.
[82] Zhang W, Thiess A, Zalden P, Zeller R, Dederichs PH, Raty JY, et al. Role of vacancies in metal–insulator transitions of crystalline phase-change materials. Nat Mater 2012;11:952–6.
[83] Zhu M, Xia M, Rao F, Li X, Wu L, Ji X, et al. One order of magnitude faster phase change at reduced power in Ti-Sb-Te. Nat Commun 2014;5:4086.

**Dr. Linggang ZHU**, Beihang University. Email: lgzhu7@buaa.edu.cn. Dr. Linggang Zhu is a lecturer at the School of Materials Science and Engineering of Beihang University, China. He got his Ph.D degree from Institute of Metal Research, Chinese Academy of Sciences in 2014. From 2010 to 2012, he was the Marie Curie Early-Stage Research Fellow at University of Edinburgh, UK. His research projects include the computation and simulation of materials properties/performance, focusing on the oxidation of engineering alloys and the oxides for RRAM application etc.

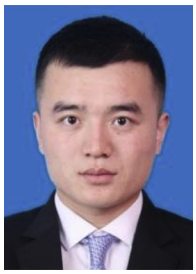

**Dr. Zhonglu GUO**, Beihang University. Email: zhongluguo@qq.com. Dr. Zhonglu Guo is currently a research assistant at Center for Integrated Computational Materials Engineering of Beihang University, China. He received his Ph.D from College of Materials, Xiamen University, in 2015. His research subjects concentrate on the electronic structures, atomic diffusion and mechanical properties of transition metal compounds, with an emphasis on their applications in RRAM, photocatalysis and flexible devices.

**Professor Jian ZHOU**, Beihang University. Email: jzhou@buaa.edu.cn. Dr. Jian Zhou is an associate professor at School of Materials Science and Engineering, Beihang University, China. He obtained his Ph.D from Institute of Metal Research, Chinese Academy of Sciences in 2003. He worked in RWTH Aachen University (Germany), Royal Institute of Technology (Sweden), Xiamen University (China), before joining Beihang University. His research interests are superalloys, intermetallics and thermoelectric materials.

**Professor Zhimei SUN**, Beihang University. Dr. Zhimei Sun is a “Chang Jiang Scholar” professor at School of Materials Science and Engineering and director of Center for Integrated Computational Materials Engineering, in Beihang University, China. She obtained her Ph.D degree in 2002 from Institute of Metal Research, Chinese Academy of Sciences. Before joining Beihang University in 2013, She worked at RWTH Aachen University (Germany), Uppsala University (Sweden) and Xiamen University (China). Her current research interests include phase-change materials for random access memory, MAX phases and high-performance metals, using both theoretical and experimental research tools. She has published more than 120 papers, with the h-index of 32.